

ternal magnetic fields  $h_x > h_1$  led to the model of oscillating motion of domain walls.<sup>2,5</sup> The basis of the model is the assumption that in external fields  $h_x > h_1$ , a spatially uniform precession of the magnetic moment is excited, with preservation of the simple and well-known functional structure of the domain wall with respect to the polar angle  $\theta$ . Application of a variational principle leads to "contraction" of the system of differential equations determining the time dependence of the variational parameters. In fields larger than the limiting field  $h_1$ , there occurs an oscillating motion of the domain wall, leading to the occurrence of a characteristic *N*-shaped variation of the mean velocity of motion of the domain wall with external field.

The existence of two essentially complementary models of the motion of domain walls in external magnetic fields indicates two possibilities for evolution of the system on attainment of the limiting values of external magnetic fields. Namely, on passage through critical

field values either definite types of stationary-profile waves may be excited, or self-neutralization of the precessional motion leads to the result that the rotation of the magnetic moment is independent of the precession. Both models lead to a decrease of the mobility of domain walls on passage through a limiting field.

<sup>1</sup>J. F. Dillon, in: Magnetism (ed. G. T. Rado and H. Sunl), Vol. 3, Academic Press, NY, 1963, p. 415.

<sup>2</sup>A. Hubert, Theorie der Domänenwände in geordneten Medien, Springer-Verlag, Berlin, 1974 (Russ. transl., "Mir", 1977).

<sup>3</sup>V. M. Eleonskii and N. N. Kirova, in: Problemy fiziki tverdogo tela (Problems of Solid State Physics) (ed. V. P. Silin), Urals Scientific Center, Academy of Sciences, USSR, Sverdlovsk, 1975, p. 184.

<sup>4</sup>V. M. Eleonskii, N. N. Kirova, and N. E. Kulagin, Zh. Eksp. Teor. Fiz. 74, 1814 (1978) [Sov. Phys. JETP 47, 946 (1978)].

<sup>5</sup>J. C. Slonczewski, Int. J. Magn. 2, 85 (1972).

Translated by W. F. Brown, Jr.

## Population and lifetime of excited states of shallow impurities in Ge

E. M. Gershenson, G. N. Gol'tsman, and N. G. Ptitsina

*V. I. Lenin State Pedagogical Institute, Moscow*

(Submitted 15 August 1978)

Zh. Eksp. Teor. Fiz. 76, 711-723 (February 1979)

An investigation was made of the dependences of the intensities of photothermal ionization lines of excited states of shallow impurities in Ge on the intensity of impurity-absorbed background radiation and on temperature. The results obtained were used to find the density and lifetime of carriers of lower excited states of the impurity centers. The lifetimes of the excited states of donors in Ge were  $10^{-9}$ - $10^{-11}$  sec and the lifetime of the lower excited state of acceptors was  $\sim 10^{-7}$  sec. In the presence of background radiation the population of the excited states was very different from the equilibrium value and, in particular, a population inversion of the  $2p_{\pm 1}$  state relative to the  $3p_0$  and  $3s$  states was observed.

PACS numbers: 71.55.Dp, 78.50.Ge, 42.50.+q

### 1. INTRODUCTION

Information on the lifetimes of excited states of impurities in semiconductors and on the distribution of nonequilibrium carriers between such excited states under various conditions is essential for the understanding of the recombination of free carriers at impurity centers, establishment of an equilibrium between impurity states and a vacant band in the case of impact ionization of impurities, optical heating of free carriers, and other experiments.

The generally accepted classical cascade recombination model of Lax,<sup>1</sup> greatly refined and developed by Abakumov *et al.*,<sup>2,3</sup> does not allow for the discrete nature of the energy spectrum of the impurity electrons. Quantum calculations<sup>4</sup> show that lower excited states may play a fairly important role in the process of electron capture but not all of them are equivalent from the

point of view of capture: for example, the states with a finite projection of the orbital momentum can be ignored. The lifetimes of excited donor states  $\tau$  calculated in these treatments amount to  $10^{-10}$ - $10^{-8}$  sec at low temperatures. Recent investigations of oscillations of the photoconductivity and photo-emf of *p*-type Ge subjected to a magnetic field<sup>5</sup> can be explained assuming anomalously long carrier lifetimes of the first excited acceptor state ( $10^{-6}$ - $10^{-7}$  sec). Even longer lifetimes (exceeding seconds) of the  $2s$  and split  $1s$  states of donors in Si are suggested by Lehto and Proctor<sup>6</sup> to explain the impurity breakdown kinetics. Such a very great difference between the values of  $\tau$  obtained using the approximate theory and indirect experimental data makes it highly desirable to determine directly the excited-state lifetimes.

The energies of transitions between excited impurity states correspond to the submillimeter wavelength range; only recently it has become possible to carry out

spectroscopic measurements at these frequencies with the necessary resolution and sensitivity: this can be done using coherent tunable oscillators in the form of backward-wave tubes. The use of such devices makes it feasible to investigate in detail the rich spectrum of excited states of shallow impurities in germanium<sup>7,8</sup> and to begin studies of the populations  $N$  of these states and of the electron lifetimes in these states.<sup>9</sup>

Our task was to determine the populations  $N$  under equilibrium and nonequilibrium conditions and use the results to find the values of  $\tau$  of the excited states in question. This is possible because the distribution of carriers between excited states under nonequilibrium conditions, for example, during optical excitation of impurities, is very different from the equilibrium distribution and depends on the lifetimes of the states involved.

We studied in detail the lower excited states of donors and in the case of acceptors only the first excited state, which was of the greatest interest because of the expected longest lifetime.<sup>5</sup> The main results are given for pure Ge samples when it is possible to ignore the effects associated with the overlap of the excited-state wave functions.

## 2. DETERMINATION OF THE POPULATIONS AND LIFETIMES OF EXCITED IMPURITY STATES FROM THE PHOTOCONDUCTIVITY SPECTRUM

Determination of the populations of excited impurity states is a difficult experimental task because the density of carriers in these states is low if the temperature is low. The most direct method is the study of the absorption spectrum representing electron transitions between excited impurity states but in the case of pure Ge samples the absorption spectra can be determined only at temperatures  $T \geq 7-8^\circ\text{K}$  (Ref. 10). The sensitivity of the measurements utilizing the photothermal ionization of excited impurity states at low temperatures is much higher than the sensitivity of the absorption measurements. However, the intensities of the individual lines in the photoconductivity spectrum cannot be used directly to determine  $N$  and  $\tau$  although such intensities carry information on the populations of the excited states. This is due to the fact that even at sufficiently low temperatures and in the case of weak photoexcitation of impurities a photothermal ionization signal of the excited states  $\Delta U$  depends not only on the population of the initial state of a given transition  $N_i$ , but also on such factors as the density  $n$  and lifetime  $\tau_c$  of free carriers in a band, and the probability  $W$  of ionization of the final state of a transition:<sup>1)</sup>

$$\Delta U = U \Delta \sigma / \sigma = U P \tau_c N_i W S_i / h \nu n S, \quad (1)$$

where  $U$  is a static bias;  $h\nu$  and  $P$  are the photon energy and power of high-frequency radiation;  $S_\lambda$  is the absorption cross section of a given transition;  $S$  is the area of the illuminated surface of the sample;  $\sigma$  and  $\Delta\sigma$  are the dc conductivity and its change due to the absorption of submillimeter radiation.

However, reliable identification of a large number of lines in the spectra representing electron transitions between excited states simplifies the problem somewhat.

Information on  $N$  and  $\tau$  was deduced by us from submillimeter photoconductivity spectra determined as a function of the intensity  $I$  of background impurity-absorbed radiation at constant temperature and from the temperature dependences obtained for a constant intensity of such radiation.

In the former case the dependence  $N(I)$  can easily be deduced from the experimental values of  $\sigma(I)\Delta U(I)$  [see Eq. (1)], because the probability of ionization  $W$  is independent of  $I$ . This is explained by the fact that  $W$  is governed by the thermal process of cascade transitions of electrons between excited impurity states followed by their arrival in a vacant band and accompanied by the absorption or emission of acoustic phonons.<sup>11</sup> If  $I$  is low, the electron density in the excited states remains in equilibrium and the product  $\sigma(I)\Delta U(I)$  is independent of  $I$ . Therefore, for low values of  $I$  we can link the experimental values of  $\sigma\Delta U$  to the thermal-equilibrium densities  $N_i$  of electrons in the appropriate excited states and to find the absolute values of  $N$  throughout the full range of the background (impurity-absorbed) radiation intensity. The equilibrium values  $N_i$  can be calculated from<sup>12</sup>

$$N_{ii} = (N_a - N_a - n) \beta_i \exp[(\epsilon_i - \epsilon_0)/kT] / \beta_0 [1 + 3 \exp(-\Delta\epsilon_0/kT)], \quad (2)$$

where  $\beta_0$  and  $\beta_i$  are the multiplicities of the degeneracy of the ground and  $i$ th levels;  $\epsilon_0$  and  $\epsilon_i$  are their binding energies;  $\Delta\epsilon_0$  is the splitting energy of the ground state.

Additional information on  $N$  can be obtained from the temperature dependences of the photoconductivity signal obtained keeping the background illumination intensity constant. However, in this case it is not possible to determine  $N$  from the temperature dependence of the intensity of a single photoconductivity line because other quantities in Eq. (1), such as  $\tau_c$ ,  $n$ , and  $W$ , also depend on  $T$ .

This difficulty can be overcome as follows. The temperature dependences are obtained for the intensities of pairs of lines which have common final but different initial states. Then, in the temperature range where the width of each line (and, consequently,  $S_\lambda$ ) is independent of  $T$ , the ratio of the intensities of such lines is proportional to the ratio of the densities in the initial states of the transitions involved and is independent of the probability of ionization of the final state or of the lifetime and density of free carriers [see Eq. (1)]. Under equilibrium conditions the ratio of the intensities is an exponential function of temperature:

$$\Delta U_i / \Delta U_j \propto N_{i1} / N_{j2} = [\beta_i \exp(\epsilon_i - \epsilon_j) / kT] / \beta_j, \quad (3)$$

whereas under nonequilibrium conditions the dependence is more complex:

$$\Delta U_i / \Delta U_j \propto N_{i1} / N_{j2} = (N_{i1} + N_{b1}) / (N_{j2} + N_{b2}), \quad (4)$$

where  $N_{b_i}$  is the nonequilibrium part of the electron density in an excited state, which depends on the intensity of the background radiation.

Having linked the experimental results for the ratio of the intensities of the photoconductivity lines at high temperatures to the equilibrium theoretical values of  $N_{T1}/$

$N_{T2}$ , we can then obtain the temperature dependence of  $N_1/N_2$  throughout the investigated range.

It follows that measurements of the intensities of various lines as a function of temperature and of the intensity of background radiation can give information on the distribution of carriers between excited states under equilibrium and nonequilibrium conditions.

The knowledge of nonequilibrium populations of the excited states in the presence of background (impurity-absorbed) radiation can then be used to determine the electron lifetimes in the lower excited states. In fact, an analysis of the calculations<sup>3,4</sup> made allowing for the energy spectrum of the excited states of shallow impurities in Ge shows that, firstly, at low temperatures  $T$  ( $\sim 4.2$  °K) the capture of electrons from a vacant band involves mainly higher excited states, and, secondly, the probability of a transition between the two closest low excited states accompanied by phonon emission is much higher than the probability of other transitions. Therefore, the recombination flux via the lower states is constant and equal to the rate of generation of carriers to the band<sup>2)</sup>  $G = n/\tau_c$ . Then, the nonequilibrium part of the population of an excited state is defined by  $N_{bi} = G\tau_i = n\tau_i/\tau_c$ . If the values of  $n$ ,  $\tau_c$ , and  $N_{bi}$  are known, we can determine the lifetimes in the low states in question. If part of the recombination flux follows a closed path bypassing a given excited state, the true values of the electron lifetime in bound states are found to be higher than those obtained as described above.

### 3. EXPERIMENTAL METHOD

Our experiments were carried out in the submillimeter wavelength ( $\lambda = 0.3-2$  mm) using a spectrometer with a backward-wave tube.<sup>7</sup> The photoconductivity spectra were determined as a function of temperature ( $T = 3-12$  °K) and the intensity  $I$  of background radiation in the impurity-absorption region. This background was provided by the warm ( $T = 300$  °K) part of the cryostat. In measurements of the line intensities  $\Delta U$  the submillimeter and background radiations reached a sample along two different metal waveguides (Fig. 1). The intensity of the background radiation reaching a sample 1 was varied in a waveguide 2 within a range of 4-5 orders of magnitude; this was done by varying the aperture in a

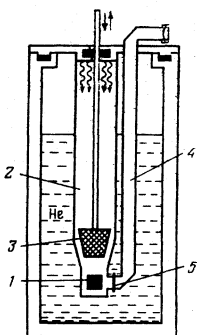


FIG. 1. Schematic diagram of the cryostat used to investigate the dependences of the intensities of the photoconductivity lines of Ge on temperature and background radiation intensity.

cold stop 3 movable in the conical part of the waveguide. In a second waveguide 4, which brought submillimeter radiation to the sample, the background radiation was almost completely suppressed by cold filters 5 (fused quartz and salt filters).

When measurements were made at a fixed submillimeter frequency corresponding to, for example, the line maximum, the dependences  $\Delta U(T, I)$  were not distorted by interference in the waveguides and in the chamber containing the sample because variation of temperature or background radiation intensity had practically no effect on the optical characteristics of the channel. The situation changed when a spectrum was recorded by scanning the submillimeter radiation frequency. In this case the high coherence of the radiation from the backward-wave tube could give rise to interference maxima and minima in the spectrum. These stray effects were suppressed by bringing submillimeter and background radiation along quasi-optic waveguides with absorbing walls and by automatic stabilization of the submillimeter power within the range of variation of the frequency of this radiation.<sup>7</sup> The intensity of background radiation was then controlled only by filters.

Under experimental conditions the resistance of a sample varied from  $10^8$  to  $10^5$   $\Omega$  depending on the background radiation. Therefore, the errors in the determination of the dependences of the line intensities on  $T$  and  $I$  were avoided by measuring the ratio of the photoconductivity signals  $\Delta U_1/\Delta U_2$  for line pairs. Both signals ( $\Delta U_1, \Delta U_2$ ) were determined for each value of  $T$  or  $I$ ; this required simultaneous use of two submillimeter spectrometers in the same experiment. Radiation from two backward-wave tubes was supplied to a given sample and the frequency of each of these tubes corresponded to a selected line of a given pair. In the course of measurement of the intensity of one line the radiation from the second backward-wave tube was suppressed.

The lifetime of free carriers was determined by measuring the dependences of the intensities of some of the photoconductivity lines on the frequency of amplitude modulation of the submillimeter radiation. Modulation at frequencies up to 10 MHz was produced by altering the voltage supplied to a backward-wave tube. A special adjustment of the position of the tube in a magnet made it possible to change from a continuous amplitude-frequency characteristic to narrow emission bands of width much less than the widths of the investigated lines. Then, variation of the anode voltage within one emission band produced sufficiently deep amplitude modulation. In these frequency measurements a sample was shunted by a resistance of 100  $\Omega$  so as to avoid distortions of the dependence of the photoconductivity signal on the modulation frequency associated with the capacitance ( $\sim 50$  pF) of the measuring circuit.

These measurements were carried out on samples of Ge:Sb and Ge:B with total impurity concentrations in the range  $10^{12}-10^{15}$   $\text{cm}^{-3}$  and with compensations of 5-20%. The samples were dumbbells, so that they could be used directly to determine the density of free carriers under various conditions from low-temperature measurements of the Hall effect.

#### 4. EXPERIMENTAL RESULTS AND DISCUSSION

1. Antimony-doped Ge exhibited more than 20 various submillimeter lines due to electron transitions between excited states.<sup>7</sup> The richness of this spectrum and its reliable identification made it possible to select suitable pairs of lines with identical or close final states, which were then used in determination of the temperature dependences. Table I gives the energies of the transitions in the photoconductivity spectrum of Ge:Sb that were used in our investigation.

Figure 2 shows, by way of example, a part of the photoconductivity spectrum of Ge:Sb for two intensities of background radiation:  $I_1$  corresponds to a practically equilibrium population of the initial states of the investigated transitions and  $I_2$  corresponds to a strongly non-equilibrium population ( $I_1 \ll I_2$ ). We can see that the ratio of the line intensities in the spectra is quite different: in the nonequilibrium situation ( $I_2$ ) the lines with the initial state  $2p_{\pm 1}$  ( $2p_{\pm 1} - 3d_{\pm 2}$ ,  $2p_{\pm 1} - 4d_0$ ) predominate.

2. Figure 3 shows, for the same values of  $I$ , the temperature dependences of the intensity ratio  $\Delta U_1/\Delta U_2$  for two pairs of lines ( $3p_0 - 3d_{\pm 1}$ ,  $2p_0 - 3d_{\pm 1}$ ) and ( $2p_{\pm 1} - 3d_{\pm 1}$ ,  $2p_0 - 5d_{\pm 1}$ ), which have different initial states but identical or close (on the energy scale) final states. Since the widths of both lines in each pair depend weakly and practically identically on  $T$  in the investigated temperature range, it follows (see Sec. 2) that for the first pair of transitions the ratio of the photoconductivity signals is proportional to the ratio of the populations of the initial states of the transitions  $N(3p_0)/N(2p_0)$ . For the second pair of transitions, we have

$$\Delta U_1/\Delta U_2 \sim N(2p_{\pm 1})W(3d_{\pm 2})/N(2p_0) \cdot W(5d_{\pm 1}).$$

Since the energies of the final states  $3d_{\pm 2}$  and  $5d_{\pm 1}$  are low and very close, we may assume that  $W(3d_{\pm 2}) \approx W(5d_{\pm 1}) \approx 1$ . This is confirmed by the temperature dependences of the ionization probability  $W$  of these excited states.<sup>10</sup> The probabilities  $W$  were investigated by selecting pairs of transitions with the same initial but different final states, so that the ratio of the line intensities was proportional to the ratio of the probabilities of ionization of the final states [see Eq. (1)]. Measurements were made

TABLE I. Energies of spectral lines and of levels participating in transitions in Ge:Sb

N	$\epsilon$ , meV	$\epsilon_n - \epsilon_m$ , meV	Transition assignment
1	0.71	1.73-1.02	$2p_{\pm 1} \rightarrow 4d_0$
2	0.74	1.48-0.74	$3d_0 \rightarrow 4p_{\pm 1}$
3	0.82	1.67-0.85	$4p_0 \rightarrow 4d_{\pm 1}$
4	0.90	1.48-0.58	$3d_0 \rightarrow 4f_{\pm 1}$
5	1.04	1.73-0.69	$2p_{\pm 1} \rightarrow 3d_{\pm 2}$
6	1.11	2.14-1.03	$3s \rightarrow 3p_{\pm 1}$
7	1.16	4.75-3.60	$2p_0 \rightarrow 2s$
8	1.23	1.73-0.50	$2p_{\pm 1} \rightarrow 5d_0$
9	1.31	2.56-1.25	$3p_0 \rightarrow 3d_{\pm 1}$
10	1.40	2.14-0.74	$3s \rightarrow 4p_{\pm 1}$
11	1.57	2.14-0.58	$3s \rightarrow 4f_{\pm 1}$
12	1.87	3.60-1.73	$2s \rightarrow 2p_{\pm 1}$
13	2.57	3.60-1.03	$2s \rightarrow 3p_{\pm 1}$
14	2.86	3.60-0.74	$2s \rightarrow 4p_{\pm 1}$
15	3.02	3.60-0.58	$2s \rightarrow 4f_{\pm 1}$
16	3.50	4.75-1.25	$2p_0 \rightarrow 3d_{\pm 1}$
17	3.90	4.75-0.85	$2p_0 \rightarrow 4d_{\pm 1}$
18	4.12	4.75-0.63	$2p_0 \rightarrow 5d_{\pm 1}$
19	4.24	4.75-0.51	$2p_0 \rightarrow 5g_{\pm 1}$

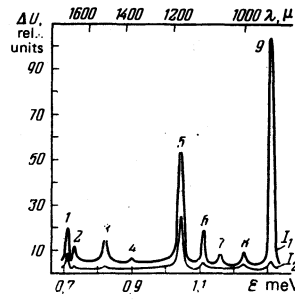


FIG. 2. Part of the photoconductivity spectrum of  $n$ -type Ge ( $N_d = 2.5 \times 10^{13} \text{ cm}^{-3}$ ,  $N_a = 1.7 \times 10^{12} \text{ cm}^{-3}$ ) recorded at two background illumination intensities ( $I_1 \ll I_2$ ) at  $T = 4.2^\circ \text{ K}$ . The numbers above the lines identify the numbers of transitions in Table I.

of the temperature dependences of the ratios of the intensities of three lines with a common initial state  $2p_{\pm 1}$  ( $2p_{\pm 1} - 4d_0$ ,  $2p_{\pm 1} - 3d_{\pm 2}$ ,  $2p_{\pm 1} - 5d_0$ ) and two lines with a common initial state  $2p_0$  ( $2p_0 - 5d_{\pm 1}$ ,  $2p_0 - 5g_{\pm 1}$ ). These measurements showed that the ratio of the ionization probabilities of the final states of these transitions was independent of  $T$  within the range  $3-10^\circ \text{ K}$ .

An analysis of the data in Fig. 3 shows that in the case of a low background radiation intensity  $I_1$  the dependences of  $\Delta U_1/\Delta U_2$  on  $1/T$  are exponential throughout the investigated temperature range, whereas for a high intensity  $I_2$ , they are exponential only at high values of  $T$ . The argument of the exponential function agrees, to within 5%, with the difference between the energies of the initial states  $\Delta \epsilon_{1,2}$  of the investigated line pairs (Table II). This is evidence of an equilibrium distribution of electrons between the excited states in the case of low background illumination intensities and high temperatures. Similar results follow also from measurements of the absorption spectra reported in Ref. 10. In this case the temperature dependences of the absorption coefficient were determined for several lines in the spectrum. All the dependences were found to be exponential and the argument of the exponential function corresponded to the energy gap between the initial and final states of the transitions.

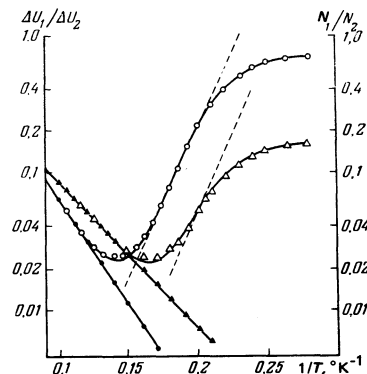


FIG. 3. Temperature dependences of the intensity ratios of two pairs of photoconductivity lines plotted for different background radiation intensities:  $\Delta U(3p_0 - 3d_{\pm 1})/\Delta U(2p_0 - 3d_{\pm 1})$  for  $I_1$  ( $\blacktriangle$ ) and  $I_2$  ( $\triangle$ );  $\Delta U(2p_{\pm 1} - 3d_{\pm 2})/\Delta U(2p_0 - 5d_{\pm 1})$  for  $I_1$  ( $\bullet$ ) and  $I_2$  ( $\circ$ ). The sample is the same as in Fig. 2.

TABLE II. Difference between energies of initial states of transitions calculated from Table I ( $\Delta\mathcal{E}'_{1,2}$ ) and from temperature dependences of line intensities ( $\Delta\mathcal{E}'_{1,2}$ )

Line pairs	$\Delta\mathcal{E}'_{1,2}$ , meV	$\Delta\mathcal{E}''_{1,2}$ , meV
$3p_0 \rightarrow 3d_{\pm 1}, 2p_0 \rightarrow 3d_{\pm 1}$	2.2	2.19
$2p_{\pm 1} \rightarrow 3d_{\pm 2}, 2p_0 \rightarrow 5d_{\pm 1}$	2.9	3.02
$4p_0 \rightarrow 4d_{\pm 1}, 2p_0 \rightarrow 4d_{\pm 1}$	3.0	3.08
$3d_0 \rightarrow 4p_{\pm 1}, 2s \rightarrow 4p_{\pm 1}$	2.1	2.12
$3s \rightarrow 4p_{\pm 1}, 2s \rightarrow 4p_{\pm 1}$	1.4	1.46

At high background illumination intensities (Fig. 3) the ratio of the photoconductivity signals in both pairs of lines passes through a minimum as a result of cooling and, beginning from a certain temperature, it tends to a constant value. In the range  $T = 6.3\text{--}4.5\text{ K}$  the temperature dependence of  $\Delta U(2p_{\pm 1} \rightarrow 3d_{\pm 2})/\Delta U(2p_0 \rightarrow 5d_{\pm 1})$  is again exponential but the argument of the exponential function is now equal to the difference between the energies of the  $2p_0$  and ground states. For the second line pair the minimum shifts toward lower temperatures and, therefore, the temperature dependence of  $\Delta U(3p_0 \rightarrow 3d_{\pm 1})/\Delta U(2p_0 \rightarrow 3d_{\pm 1})$  in the range  $5.5\text{--}4.2\text{ K}$  is nonexponential.

The existence of a minimum in the temperature dependences of the ratio  $\Delta U_1/\Delta U_2$  shows that the populations of the states  $2p_{\pm 1}$  and  $3p_0$  become nonequilibrium, beginning from  $T \approx 7$  and  $6\text{ K}$ , respectively. The rise of the ratio  $\Delta U_1/\Delta U_2$  as a result of lowering of  $T$  and the exponential nature of the dependence  $\Delta U_1/\Delta U_2$  on  $1/T$  for the first line pair show that the population of the state  $2p_0$  remains in equilibrium to much lower temperatures than  $2p_{\pm 1}$  and  $3p_0$ . The region of the plateau in the dependence of  $\Delta U_1/\Delta U_2$  on  $1/T$  for both line pairs begins at the same temperature of  $\approx 3.8\text{ K}$ . Below this temperature the populations of all the initial states of the investigated transitions are governed entirely by the background illumination.

The equilibrium nature of the electron distribution between the excited states at high temperatures allows us to link the experimental values of  $\Delta U_1/\Delta U_2$  to the equilibrium values of  $N(2p_{\pm 1})/N(2p_0)$  and  $N(3p_0)/N(2p_0)$  for the line pairs in question. We must bear in mind that in the limit  $T \rightarrow \infty$ , we have  $N(3p_0)/N(2p_0) = 1$  and  $N(2p_{\pm 1})/N(2p_0) = 2$ , because the multiplicity of degeneracy of the level  $2p_{\pm 1}$  is twice as high as the multiplicity of degeneracy of the levels  $2p_0$  and  $3p_0$ . The scale of relative densities obtained in this way is shown on the right of Fig. 3. We can see that in the limit of low temperatures, when the populations of the initial states  $2p_{\pm 1}$ ,  $3p_0$ , and  $2p_0$  are not in equilibrium, we have  $N(3p_0)/N(2p_0) = 0.16$  and  $N(2p_{\pm 1})/N(2p_0) = 0.7$ .

It is interesting to note that the ionization energy of the  $2p_{\pm 1}$  state is less than that of the  $3p_0$  state and that under equilibrium conditions we have  $N(2p_{\pm 1})/N(3p_0) = 0.2$  at  $T = 4.2\text{ K}$ . Under nonequilibrium conditions, we find that  $N(2p_{\pm 1})/N(3p_0) = 4.2$ , i.e., a population inversion of the  $2p_{\pm 1}$  state relative to the lower state  $3p_0$  (and also relative to the  $3s$  state) is observed.

The exponential temperature dependence of the ratio

$\Delta U(2p_{\pm 1} \rightarrow 3d_{\pm 2})/\Delta U(2p_0 \rightarrow 5d_{\pm 1})$  observed at low temperatures makes it possible to determine not only the relative values of the nonequilibrium densities of electrons in the initial states of the investigated transitions but also the absolute values of these densities throughout the investigated temperature range; this information is obtained by calculating the equilibrium population of the level  $2p_0$  in the temperature range  $6\text{--}4.8\text{ K}$  and applying Eqs. (2) and (4). The nonequilibrium values  $N(2p_{\pm 1})$  and  $N(3p_0)$  obtained in this way are found to be independent of temperature right up to  $T \approx 7\text{ K}$ , which is evidence of the constancy of the lifetime of electrons in the  $2p_{\pm 1}$  and  $3p_0$  states at these temperatures.

3. Information on the nonequilibrium distributions of carriers between the excited states deduced from the temperature dependences is fully supported by studies of the dependences of the intensities of the same lines on the background radiation intensity at a constant temperature. Figure 4 shows the dependences of the intensity ratios of two line pairs

$$\Delta U(2p_{\pm 1} \rightarrow 3d_{\pm 2})/\Delta U(3p_0 \rightarrow 3d_{\pm 1}) \sim N(2p_{\pm 1})/N(3p_0),$$

$$\Delta U(2p_{\pm 1} \rightarrow 3d_{\pm 2})/\Delta U(2p_0 \rightarrow 3d_{\pm 1}) \sim N(2p_{\pm 1})/N(2p_0)$$

on the dc conductivity  $\sigma$ , which—at  $T = 4.2\text{ K}$  and for the background radiation intensities employed—is proportional to the generation-recombination flux  $G$  and, consequently, to the background radiation intensity  $I$ .

We can see that when the background radiation intensity is low, the ratio  $\Delta U_1/\Delta U_2$  for both line pairs depends weakly on this intensity. Under these conditions the populations of the states  $2p_0$ ,  $3p_0$ , and  $2p_{\pm 1}$  are close to equilibrium, which follows also from the temperature dependences for  $I = I_1$  plotted in Fig. 3. Therefore, the experimental values of  $\Delta U_1/\Delta U_2$  can be linked to the calculated, from Eq. (3), values of  $N_1/N_2$  at a given temperature (the scale on the right in Fig. 4). When the background radiation intensity is higher, the value of  $N_1/N_2$  rises for both line pairs and we have  $N(2p_{\pm 1})/N(2p_0) \sim G$  in a certain range of the generation-recombination flux. Clearly, the carrier density in the  $2p_0$  state does not change, whereas in the  $2p_{\pm 1}$  state it rises proportionally to the flux. Finally, beginning from some value of  $G$ ,  $N_1/N_2$  ceases to vary. In this range the populations of all the initial states of the investigated line pairs are completely nonequilibrium and proportional to  $G$ . The experimental values of the ratio  $N_1/N_2$  in the region of the plateau are  $N(2p_{\pm 1})/N(2p_0) = 0.68$  and  $N(2p_{\pm 1})/N(3p_0) = 3.8$ , in good agreement with the values obtained above from the temperature dependences.

Information deduced from Fig. 4 can be used to find the dependence of the populations of the excited states on the generation-recombination flux (Fig. 5). It is clear that the populations of the  $2p_0$ ,  $3p_0$ , and  $2p_{\pm 1}$  states depend in different ways on  $G$ . For example, the population of the  $2p_0$  state is in equilibrium right up to  $G \approx 10^{15}\text{ cm}^{-3} \cdot \text{sec}^{-1}$  and the populations of the  $2p_{\pm 1}$  and  $3p_0$  states is governed by the background radiation intensity for  $G > 10^{12}$  and  $10^{13}\text{ cm}^{-3} \cdot \text{sec}^{-1}$ , respectively.

4. The known excited-state populations under nonequilibrium conditions can now be used to estimate the carrier lifetime  $\tau$  in these excited states. The value of the

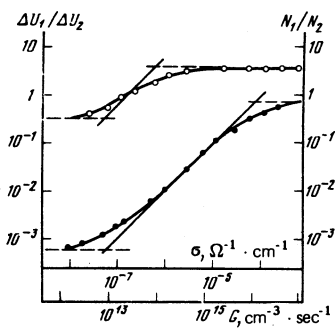


FIG. 4. Dependences of the intensity ratios of two pairs of photoconductivity lines on the generation-recombination flux at  $T = 4.2^\circ \text{K}$ :  $\Delta U(2p_{\pm 1} \rightarrow 3d_{\pm 2})/\Delta U(3p_0 \rightarrow 3d_{\pm 1})$  ( $\circ$ );  $\Delta U(2p_{\pm 1} \rightarrow 3d_{\pm 2})/\Delta U(2p_0 \rightarrow 3d_{\pm 1})$  ( $\bullet$ ). The same sample as in Fig. 2.

free-carrier density  $n$  corresponding to a given background radiation intensity is required in these calculations (Sec. 2); it can be obtained from the Hall effect, whereas the lifetime can be found from the dependence of the photoconductivity signal  $\Delta U$  of any one of the investigated lines on the frequency  $\Omega$  of amplitude modulation of the submillimeter radiation. The values of  $\Delta U(\Omega)$  obtained in this way fit well the dependence

$$\Delta U(\Omega) = \Delta U(0) (1 + \Omega^2 \tau_r^2)^{-1/2}.$$

It follows that the photoconductivity kinetics is described by a specific relaxation time  $\tau_r$ . This relaxation time is the same for all the lines in the spectrum, i.e., the details of the ionization process are not manifested in these experiments, and  $\tau_r$  is governed only by the process of free-carrier capture. However, additional measurements (which are outside the scope of the present paper and will be published later) showed that  $\tau_r$  is not always identical with  $\tau_c$ . If the impurity concentration is high and temperature is low,  $\tau_r$  may be considerably greater than  $\tau_c$ . However,  $\tau_r$  and  $\tau_c$  are related so that we can use the measured values of  $\tau_r$  to find  $\tau_c$ .<sup>3)</sup> For example, for the sample whose characteristics are plotted in Figs. 2–5, we have  $\tau_r = 2.3 \times 10^{-7}$  sec and  $\tau_c = 5 \times 10^{-8}$  sec.

Measurements of  $\tau_c$  and  $n$  make it possible to determine the absolute values of the generation-recombination flux  $G$  (lower scale in Figs. 4 and 5). We can then calcu-

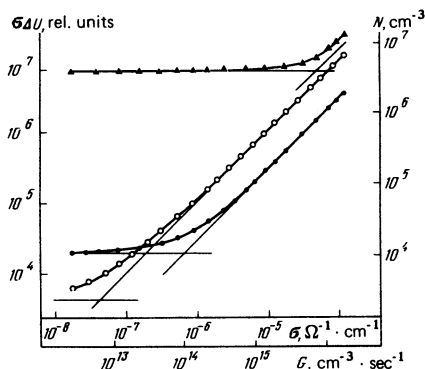


FIG. 5. Dependences of  $\sigma \Delta U$  on  $G$  at  $T = 4.2^\circ \text{K}$  for the following transitions:  $2p_0 \rightarrow 3d_{\pm 1}$  ( $\blacktriangle$ ),  $3p_0 \rightarrow 3d_{\pm 1}$  ( $\bullet$ ), and  $2p_{\pm 1} \rightarrow 3d_{\pm 2}$  ( $\circ$ ). The same sample as in Fig. 2.

late the excited-state lifetimes from Fig. 5. For example, for  $G = 10^{17} \text{cm}^{-3} \cdot \text{sec}^{-1}$ , when the levels  $2p_0$ ,  $3p_0$ , and  $2p_{\pm 1}$  have nonequilibrium populations, the free-carrier density is  $5 \times 10^9 \text{cm}^{-3}$ , and the densities and lifetimes of electrons in these states are, respectively,  $6 \times 10^7$ ,  $10^7$ , and  $4 \times 10^7 \text{cm}^{-3}$  and  $6 \times 10^{-10}$ ,  $10^{-10}$ , and  $4 \times 10^{-10}$  sec.

5. A similar procedure was used to determine the values of  $N$  and  $\tau$  for all the lower excited states of donors. Measurements were made of the temperature dependences of the ratio of the intensities of the following line pairs:  $4p_0 - 4d_{\pm 1}$  and  $2p_0 - 4d_{\pm 1}$ ;  $3d_0 - 4p_{\pm 1}$  and  $2s - 4p_{\pm 1}$ ;  $3s - 3p_{\pm 1}$  and  $2s - 3p_{\pm 1}$ . At low background radiation intensities the dependences of  $\Delta U_1/\Delta U_2$  on  $1/T$  were exponential for all line pairs and the argument of the exponential function was equal to the difference between the energies of the initial states of the selected pair of transitions  $\Delta \epsilon_{1,2}'$ . Table II gives the values of  $\Delta \epsilon_{1,2}'$  obtained in this way and the values of  $\Delta \epsilon_{1,2}''$  calculated from Table I. The agreement between these two sets of values (within the limits of the experimental error) shows that in the case of weak background illumination all the low excited states of donors in Ge have equilibrium populations.

Measurements of the dependences of  $\Delta U_1/\Delta U_2$  on the background radiation intensity were carried out for other pairs of lines starting from transitions involving the same low excited states:  $3p_0 - 3d_{\pm 1}$  and  $2s - 2p_{\pm 1}$ ;  $3s - 3p_{\pm 1}$  and  $3p_0 - 3d_{\pm 1}$ ;  $3d_0 - 4p_{\pm 1}$  and  $2s - 4p_{\pm 1}$ ;  $4p_0 - 4d_{\pm 1}$  and  $2p_{\pm 1} - 3d_{\pm 2}$ . Fundamental difficulties limiting the experimental possibilities were encountered in the course of these measurements. An increase in the background illumination intensity in a situation when the populations of the initial states were still in equilibrium reduced the line intensities (Fig. 2), which was simply due to an increase in the conductivity of the sample. The weakest lines were then no longer visible against the nonresonant photoconductivity. Therefore, the measurements carried out on the  $4p_0$  and  $3d_0$  states could be used only to estimate the upper limits of the values of  $\tau$ .

Some difficulties were also found when  $\tau$  was determined for the  $2s$  state using the  $2s - 2p_{\pm 1}$  transition. Since the lifetime of the  $2p_{\pm 1}$  state was long, the carrier densities in the  $2p_{\pm 1}$  and  $2s$  states were similar at high illumination intensities and the value of  $\Delta U(2s - 2p_{\pm 1})$  was proportional not to  $N(2s)$  but to  $N(2s) - \frac{1}{2}N(2p_{\pm 1})$  (the factor  $\frac{1}{2}$  appeared because of the different multiplicities of degeneracy of the  $2s$  and  $2p_{\pm 1}$  states). The value of  $\tau(2s)$  was found by determining the dependence of  $\Delta U(3p_0 - 3d_{\pm 1})/\Delta U(2s - 2p_{\pm 1})$  on  $G$ . At low background illumination intensities the ratio  $\Delta U_1/\Delta U_2$  was linked to the calculated equilibrium value of  $N(3p_0)/N(2s)$ . Then, under nonequilibrium conditions the limiting value of  $N(3p_0)/[N(2s) - \frac{1}{2}N(2p_{\pm 1})]$  was 1.25. Since under the same conditions we found that  $N(2p_{\pm 1})/N(3p_0) = 3.6$  (Fig. 4), we concluded that  $N(2s)/N(2p_{\pm 1}) = 0.72$  and  $\tau(2s) = 3.2 \times 10^{-10}$  sec.

Table III gives the ratios of the carrier densities in the initial states of the investigated transition pairs under equilibrium and strongly nonequilibrium conditions. The values of  $\tau$  of all the investigated states of Sb donors in

TABLE III. Ratio of electron densities in initial states of transitions under equilibrium and nonequilibrium conditions ( $T = 4.2^\circ \text{K}$ )

Transition pairs	$N_i/N_s$	
	equilibrium conditions	nonequilibrium conditions
$2p_{\pm 1} \rightarrow 3d_{\pm 2}, 2p_0 \rightarrow 3d_{\pm 1}$	$5 \cdot 10^{-4}$	0.7
$2p_{\pm 1} \rightarrow 3d_{\pm 2}, 3p_0 \rightarrow 3d_{\pm 1}$	0.2	3.6
$3s \rightarrow 3p_{\pm 1}, 3p_0 \rightarrow 3d_{\pm 1}$	0.31	0.6
$3p_0 \rightarrow 3d_{\pm 1}, 2s \rightarrow 2p_{\pm 1}$	$5.6 \cdot 10^{-2}$	0.3

Ge are as follows:

states:	$2p_0$	$2s$	$3p_0$	$3s$	$2p_{\pm 1}$	$4p_0$	$3d_0$
$\tau \cdot 10^{10}, \text{sec.}$	6	3.2	1	0.6	$\frac{4}{4}$	$< 0.4$	$< 0.4$

For the first excited state (8-01) of the B acceptor we have  $\tau = 6 \times 10^{-8}$  sec. We can see that the lifetime of the  $2p_{\pm 1}$  state exceeds  $\tau$  of not only the higher  $4p_0$  and  $3d_0$  states but also of the lower  $3p_0$  and  $3s$  states. This is clearly due to the fact that the  $2p_{\pm 1}$  state is the lowest on the energy scale among the levels with a finite projection of the momentum and a phonon transition from this level to lower ones is difficult.

The long lifetime in the  $2p_{\pm 1}$  state explains why the dominant lines in the spectrum of Fig. 2 are  $2p_{\pm 1} - 4d_0$ ,  $2p_{\pm 1} - 3d_{\pm 2}$ , and  $2p_{\pm 1} - 5d_0$ . Under nonequilibrium conditions the initial state of these transitions is more highly populated than the states  $3p_0$ ,  $3s$ ,  $3d_0$ , and  $4p_0$  which are the initial states for other lines in this part of the spectrum.

6. All the experimental results and their analysis have been made so far for a typical fairly pure sample of  $n$ -type Ge. We shall now consider the results of measurements of the dependences of the intensities of the submillimeter photoconductivity lines on the intensity of the background illumination for a batch of samples of  $n$ -type Ge with different donor concentrations ( $N_d = 10^{12} - 2 \times 10^{14} \text{ cm}^{-3}$ ) and different degrees of compensation ( $N_a/N_d = 0.05 - 0.3$ ). We shall also consider the features typical of  $p$ -type Ge.

The dependences  $\Delta U(I)$  for each line in the spectrum are found to be identical for all the samples under the same illumination conditions. This shows that the electron lifetime in the investigated excited states is independent of the impurity concentration right up to  $N_d \approx 10^{14} \text{ cm}^{-3}$ .

The accumulated information on the values of  $N$  and  $\tau$  for the donor states can now be used to determine the lifetime of holes in the first excited acceptor state without carrying out all the measurements of the carrier density in various excited states and also of the density and lifetime of free carriers. The lifetime of the first excited acceptor state was determined by comparing the dependences of the intensities of the lines at 2.44 meV (8-01-7-0 transition)<sup>8</sup> of the acceptor B in Ge and of the 1.04 MeV line ( $2p_{\pm 1} - 3d_{\pm 2}$ ) of the Sb donor in Ge on the intensity of the background illumination in the case of the same illumination of both samples at  $T = 4.2^\circ \text{K}$ . In this case the ratio of the generation-recombination fluxes in the samples was equal to the ratio of the concentrations of the neutral centers because the cross sec-

tions for the absorption of the background radiation by B and Sb were practically the same. Hence, we concluded that the ratio of the carrier densities under nonequilibrium conditions at the 8-01 level (in  $p$ -type Ge) and at the  $2p_{\pm 1}$  level (in  $n$ -type Ge) was  $N(8-01)/N(2p_{\pm 1}) = (N_a - N_d)\tau(8-01)/(N_d' - N_d') \cdot \tau(2p_{\pm 1})$ . Experiments indicated that the ratio of the intensities of the 2.44 and 1.04 meV lines was practically independent of the background illumination intensity, although for each of these lines the dependence  $\Delta U(G)$  was the same as in Fig. 5. Therefore, when  $I$  was varied, the density ratio  $N(8-01)/N(2p_{\pm 1})$  remained the same under equilibrium conditions and could be calculated from Eq. (2):

$$\tau(8-01)/\tau(2p_{\pm 1}) = (\beta_1\beta_{02}/\beta_2\beta_{01})(1+3 \exp \Delta \epsilon_0/kT) \exp(\epsilon_1 - \epsilon_0)/(\epsilon_2 - \epsilon_0)$$

and, consequently,  $\tau(8-01) = 6 \times 10^{-8}$  sec. Thus, the lifetime in the first excited acceptor state was found to be two orders of magnitude higher than in the first excited donor state. This was in agreement with the estimates in Ref. 13.

The dependence of the lifetime on the concentration of the main impurity was determined for the first excited acceptor state in the same way as for the donor and this was done in the range  $N_a = 10^{12} - 5 \times 10^{15} \text{ cm}^{-3}$  and  $N_d/N_a \leq 0.05$ . It was found that in the case of the acceptors the value of  $\tau$  once again was independent of the impurity concentration. The high value of  $\tau$  of the first excited acceptor state made it desirable to investigate also  $p$ -type Ge with higher values of  $N_a$  but it was found that a strong broadening suppressed the investigated line as soon as  $N_a \approx 5 \times 10^{15} \text{ cm}^{-3}$  was reached.

7. We shall now compare the lifetimes of the excited donor states with the values of  $1/\Delta\omega$  ( $\Delta\omega$  is the line half-width and  $\omega$  is the frequency) for the photothermal ionization lines of the excited donor states in pure Ge samples.<sup>7</sup> Such a comparison is justified since one of the mechanisms broadening the impurity line is the interaction between bound electrons and phonons that determines, in particular, the electron lifetime in the initial and final states of each transition. In the case of pure Ge samples this mechanism is clearly predominant. The line width is then governed by the shorter of the lifetimes, i.e., usually by the lifetime of the final state of the transition. The widths of the various lines in the spectra of such samples are  $1/\Delta\omega = (2.6 - 0.6) \times 10^{-10}$  sec at low temperatures, i.e., they are quite close to our lifetimes  $\tau$  of the high excited states.

## 5. CONCLUSIONS

One should note a number of new facts which have to be allowed for in discussing various low-temperature phenomena in semiconductors.

The populations of the excited states of shallow impurities in Ge at  $T \approx 5^\circ \text{K}$  differs considerably from equilibrium even when the intensity of the background radiation is low (such radiation is usually present in various experiments at helium temperatures). For example, under equilibrium conditions the carrier density in the first excited donor state in Ge is 3-4 orders of magnitude greater than the population of the higher states, whereas in the presence of the background radiation the populations are almost equal and the  $2p_{\pm 1}$  state exhibits

a population inversion relative to the  $3p_0$  and  $3s$  states.

In the case of doped Ge samples with the concentration of the capture centers  $\geq 10^{14} \text{ cm}^{-3}$  the free-carrier lifetimes are comparable with the lifetimes of the lower excited donor states ( $\sim 10^{-9}$  sec). In the case of the acceptors the lifetime of the first excited state ( $\sim 10^{-7}$  sec) is considerably greater than  $\tau_c$ . Therefore, in the case of photoexcitation the population of the excited states becomes considerable compared with the free-carrier density. Clearly, this should be allowed for specially in the theory of carrier recombination at Coulomb impurity centers in semiconductors because usually the distribution function of nonequilibrium carriers in the range of negative energies obeying  $|\varepsilon| \gg kT$  is assumed to be zero. The same problem arises in a discussion of the dependence of the free-carrier lifetime on the electric field under impurity breakdown conditions because the relatively long lifetimes of the excited impurity states are responsible for their strongly nonequilibrium populations under these conditions too.

<sup>1</sup>Low temperatures and weak photoexcitation conditions allow us to ignore the population of the final state  $N_f$  and the probability of ionization of the initial state  $W_i$ . In the more general case,  $N_i$  in Eq. (1) should be replaced with  $(N_i - N_f)$  and  $W$  should be changed to  $(W - W_i)$ . In particular, such a substitution should be made in Sec. 4.5.

<sup>2</sup>Direct carrier release from the ground to excited states of impurities by room-temperature background radiation is slight. This is due to a reduction in the background radiation intensity at longer wavelengths and also due to the width of the photoionization band ( $\sim 5$  MeV) being much greater than the width of the lines of the transitions in the investigated samples (0.1–0.2 MeV). Therefore, although the absorption cross section for the  $1s \rightarrow 2p_{x1}$  transition (the most interesting in the spectrum) is several times greater than the photoionization cross section, even in this case the direct release of carriers is less than the overall release to a vacant band.

<sup>3</sup>In Ref. 9 we published the preliminary results and identified  $\tau_r$  with  $\tau_c$ , as is usually done. Therefore, the absolute values of  $\tau$  were somewhat overestimated.

<sup>1</sup>M. Lax, Phys. Rev. **119**, 1502 (1960).

<sup>2</sup>V. N. Abakumov and I. N. Yassievich, Zh. Eksp. Teor. Fiz. **71**, 657 (1976) [Sov. Phys. JETP **44**, 345 (1976)].

<sup>3</sup>V. N. Abakumov, V. I. Perel', and I. N. Yassievich, Zh. Eksp. Teor. Fiz. **72**, 674 (1977) [Sov. Phys. JETP **45**, 354 (1977)]; Fiz. Tekh. Poluprovodn. **12**, 3 (1978) [Sov. Phys. Semicond. **12**, 1 (1978)].

<sup>4</sup>G. Ascarelli and S. Rodriguez, J. Phys. Chem. Solids **22**, 57 (1961); R. A. Brown and S. Rodriguez, Phys. Rev. **153**, 890 (1967); F. Belezny and G. Pataki, Phys. Status Solidi **13**, 499 (1966).

<sup>5</sup>V. F. Gantmakher and V. N. Zverev, Zh. Eksp. Teor. Fiz. **71**, 2314 (1976) [Sov. Phys. JETP **44**, 1220 (1976)].

<sup>6</sup>A. Lehto and W. G. Proctor, J. Phys. C **10**, L481 (1977).

<sup>7</sup>E. M. Gershenson, G. N. Gol'tsman, and N. G. Ptitsina, Zh. Eksp. Teor. Fiz. **64**, 587 (1973) [Sov. Phys. JETP **37**, 299 (1973)]; E. M. Gershenson, G. N. Gol'tsman, and A. I. Elant'ev, Zh. Eksp. Teor. Fiz. **72**, 1062 (1977) [Sov. Phys. JETP **45**, 555 (1977)].

<sup>8</sup>E. M. Gershenson, G. N. Gol'tsman, and M. L. Kagane, Zh. Eksp. Teor. Fiz. **72**, 1466 (1977) [Sov. Phys. JETP **45**, 769 (1977)].

<sup>9</sup>E. M. Gershenson, G. N. Gol'tsman, and N. G. Ptitsina, Pis'ma Zh. Eksp. Teor. Fiz. **25**, 574 (1977) [JETP Lett. **25**, 539 (1977)].

<sup>10</sup>E. M. Gershenson, L. A. Orlov, and N. G. Ptitsina, Pis'ma Zh. Eksp. Teor. Fiz. **22**, 207 (1975) [JETP Lett. **22**, 95 (1975)]; E. M. Gershenson, G. N. Gol'tsman, L. A. Orlov, and N. G. Ptitsina, Proc. Thirteenth Intern. Conf. on Physics of Semiconductors, Rome, 1976, publ. by North-Holland, Amsterdam (1976), p. 631.

<sup>11</sup>Sh. M. Kogan and B. I. Sedunov, Fiz. Tverd. Tela (Leningrad) **8**, 2382 (1966) [Sov. Phys. Solid State **8**, 1898 (1967)].

<sup>12</sup>J. S. Blakemore, Semiconductor Statistics, Pergamon Press, Oxford, 1962 (Russ. Transl., Mir, M., 1964).

<sup>13</sup>V. F. Gantmakher, V. N. Zverev, S. V. Meshkov, and É. I. Rashba, Izv. Akad. Nauk SSSR Ser. Fiz. **42**, 1160 (1978).

Translated by A. Tybulewicz